

The Photovoltage-Determining Mechanism in Dye-Sensitized Solar Cells

François Pichot and Brian A. Gregg*

National Renewable Energy Laboratory, 1617 Cole Boulevard, Golden, Colorado 80401-3393

Received: August 25, 1999; In Final Form: November 19, 1999

We attempt to distinguish between two competing models of the photovoltage-determining mechanism in dye-sensitized solar cells. One model does not consider the equilibrium potential difference at the TiO_2 /substrate interface to be a significant factor in determining the photovoltage; the other claims that this potential difference sets the upper limit to the achievable photovoltage. We deposit dye-sensitized TiO_2 films on four different substrates that have vacuum work functions spanning a 1.4 eV range and measure the photovoltage obtained from these films in three different redox electrolyte solutions. No significant differences in photovoltage are obtained on the different substrates, not even on Pt where the interfacial potential should oppose electron transfer. We suggest that the interfacial potential barrier may be smaller than expected and/or too thin to have a significant influence on cell performance. We conclude that the photovoltage is determined by photoinduced chemical potential gradients, not by equilibrium electric fields.

Background

Dye-sensitized solar cells^{1–4} are the most promising alternative to conventional solar cells conceived in recent years. These unusual cells combine aspects of semiconductor photoelectrochemistry, dye-sensitization, and colloid chemistry in a mix that is not yet fully understood and probably far from optimized. Even the most fundamental aspect of the dye cells—how they generate a photovoltage and thereby a photovoltaic effect—is still controversial. In this Letter we discuss the two competing models of the photovoltage-determining mechanism and present experiments that we believe distinguish between them.

We first briefly summarize the points of agreement between the two models, and among most of the involved researchers: Both models assume that the initial charge separation (photo-injection of electrons from the dye into the nanocrystalline TiO_2 film and transfer of “holes” into solution) is primarily a kinetically controlled process^{3,5} and that the subsequent electron transport through the bulk of the film occurs in an essentially electric field-free regime, that is, it occurs by diffusion rather than by field-driven drift.^{3,6–12} There are no significant electric fields in the individual nanocrystalline TiO_2 particles^{1,7} or between the sintered particles in the bulk of the film^{9,13–15} because, in the first case, the particles are too small (~ 15 nm) and too lightly doped to support a significant space charge and because, in the second case, the sintered particles are surrounded by a concentrated electrolyte solution that screens any existing electric fields within about a nanometer.

The models differ, however, in how they treat the significance of an equilibrium interfacial electrical potential gradient at the TiO_2 /substrate interface, and therefore invoke somewhat different forces to drive photoinjected electrons across this interface. The earlier model, that we refer to as the “kinetic model”, was developed by a number of groups^{3,6–9,14–21} but often appears in the literature as a common understanding rather than as a clearly formulated model. It posits that the photoinjected electrons are driven into the substrate electrode by the chemical potential gradient created by the photoinduced increase

in the concentration of electrons in the TiO_2 relative to the substrate electrode. That is, the quasi Fermi level for electrons, which by definition is equal in the SnO_2 and TiO_2 at equilibrium, becomes more negative in the TiO_2 when electrons are photo-injected from the excited dye molecules. The electrical potential gradient that would otherwise develop between the photoinjected electrons and the oxidized species, and would oppose charge separation, is electrostatically screened by the electrolyte solution that permeates the bulk of the nanocrystalline TiO_2 film.⁹ Therefore, the photoinduced gradient of the quasi Fermi level consists almost entirely of a chemical potential gradient. (Without the electrostatic screening by the electrolyte, and without the band-bending that drives charge separation in nonporous dye-sensitized electrodes, most photoinjected electrons would not escape from their “image” charges and would recombine before reaching the substrate electrode.^{9,22,23}) The photoinduced difference in electrochemical potential across the nanocrystalline TiO_2 /electrolyte interface (the difference between the quasi Fermi level for electrons in the TiO_2 and the quasi Fermi level for “holes” in solution) sets an upper limit to the photovoltage, V_{oc} , since it is this difference, and the fact that electrons and holes are confined to separate chemical phases, that drives electrons toward the substrate electrode and holes toward the counter electrode. The actual value of V_{oc} will be less than this value because of recombination processes, electrochemical overpotentials, etc. This model does not consider the existence of an equilibrium electrical potential difference between the TiO_2 film and the SnO_2 substrate. We should note that this description represents our understanding of the kinetic model and does not appear verbatim in any of the referenced papers.

The other model, the “junction model”,¹² is newer and not so thoroughly elaborated as the kinetic model. In many ways it is analogous to the model of a conventional solid-state solar cell. It posits the existence of a large equilibrium electric field (band bending) at the TiO_2 / SnO_2 interface that drives charge separation across the interface. The junction potential is determined by the difference between the work function of the substrate electrode, Φ_{sub} , and the solution redox potential, Φ_{redox} ,

* Corresponding author.

in the same fashion as a junction is formed at a conventional semiconductor electrode upon immersion in a redox electrolyte solution.²⁴ However, the junction potential in the dye cell is restricted to a very narrow region (~ 20 nm) at the $\text{TiO}_2/\text{SnO}_2$ interface because the electrolyte solution that permeates the porous TiO_2 film would screen an electric field within ~ 1 nm or so anywhere else in the cell.^{9,12} Therefore, the junction potential does not drive charge transport through the bulk of the TiO_2 , which remains electric field-free, but only across the $\text{TiO}_2/\text{SnO}_2$ interface. It is assumed that the separation of the electrostatically screened, photoinjected electrons in the TiO_2 from their image charges in solution cannot occur without this interfacial electrical potential gradient. Therefore, the magnitude of this equilibrium potential difference sets the upper limit to the magnitude of the achievable photopotential.¹²

There is another aspect of the junction model that was not discussed in its original presentation but is relevant to our comparison of the two models: upon illumination, a chemical potential gradient is formed in a fashion identical to that in the kinetic model. This is unavoidable, and a similar process occurs in conventional p–n junction solar cells. Therefore, this model assumes a combined electrical and chemical potential gradient as the thermodynamic driving force that drives electrons across the $\text{TiO}_2/\text{SnO}_2$ interface. Furthermore, it asserts that it is not possible to drive electrons across this interface without the electrical potential gradient; that is, a chemical potential gradient by itself (as in the kinetic model) is not sufficient.¹² Other groups have deduced the existence of,^{19,25} or modeled,²⁶ a junction potential occurring at the $\text{TiO}_2/\text{SnO}_2$ interface but did not estimate its magnitude or claim it sets an upper limit to V_{oc} . One group claims to have “measured” a barrier height of 0.67 V by fitting, without attempting to justify the procedure, the current–voltage behavior of dye cells to the equations valid for solid-state p–n junctions.²⁷

The generalized thermodynamic driving force in solar cells is the gradient of the electrochemical potential; these gradients drive the fluxes of electrons and holes. Whether the electrochemical potential gradient consists of a chemical potential difference, an electrical potential difference, or a mixture of the two is unimportant from a thermodynamic perspective. As an example relevant to this discussion, there is general agreement that the flux of “holes” (primarily I_3^-) through solution to the counter electrode in the dye cells is driven by a pure chemical potential gradient. No significant electric fields can exist in concentrated electrolyte solution, yet I_3^- ions reach the electrode surface and are reduced at a high rate with minimal overpotential. The kinetic model, in essence, assumes that the flux of electrons through the nanocrystalline TiO_2 to the opposite electrode occurs by a similar mechanism, thus resulting in a photovoltaic effect in the absence of any significant electric fields (except across the Helmholtz layers). The junction model, in contrast, assumes that the flux of electrons to the substrate electrode is a fundamentally different process than the flux of I_3^- to the counter electrode, because the separation of electrons from their screening ions at the substrate can occur only with the assistance of an electric field whereas no such field is required to separate the I_3^- ions, or other redox species, from their screening ions at the counter electrode.

As far as we can tell, both models can adequately account for the existing experimental results, so new experiments to distinguish between them are needed. The difference between the work function of the substrate electrode and the solution redox potential, $\Phi_{\text{sub}} - \Phi_{\text{redox}}$, sets the upper limit to V_{oc} in the junction model, while this factor is not considered in the kinetic

model. So changing this difference and monitoring its effect on the photovoltage seems like the clearest way to distinguish between the models. Here we report measurements of V_{oc} obtained from dye-sensitized TiO_2 films deposited on four different substrates that have vacuum work functions spanning a 1.4 eV range.

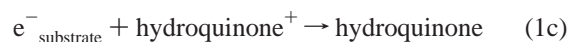
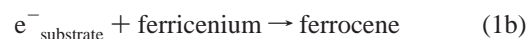
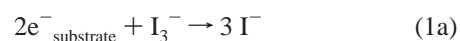
Experimental Section

Electrodes. The electrodes are Sn-doped In_2O_3 , or ITO (Delta Technologies), F-doped SnO_2 (Libbey Owens Ford), Au (prepared by sequential evaporation of 500 Å Cr, 600 Å Pd, and 1000 Å Au onto a clean glass substrate), and Pt (prepared by sequential evaporation of 600 Å Ti and 400 Å Pt; these were also used as counter electrodes). Versus vacuum, the work functions of the clean electrodes are $\Phi_{\text{ITO}} \approx 4.3$ eV,²⁸ $\Phi_{\text{SnO}_2} \approx 4.8$ eV,²⁸ $\Phi_{\text{Au}} \approx 5.1$ eV²⁹ and $\Phi_{\text{Pt}} \approx 5.7$ eV.²⁹ The electrochemical reference electrode that we use, SCE, is ≈ 4.75 eV vs vacuum.²⁴ The TiO_2 colloids and the films on SnO_2 , Au, and Pt substrates were prepared by the methods described earlier.³⁰ Since ITO is not stable at the high temperatures (450 °C) used in the normal film preparation technique, films on this substrate were prepared by a low-temperature method.³¹ The dye, *cis*-di(thiocyanato)bis(2,2'-bipyridine-4,4'-dicarboxylato)ruthenium(II), N3 (Solaronix), was adsorbed from ethanol solution for 12 h and the films were then soaked in pure ethanol for 12 h to remove any excess dye.

Measurements. We could not use the normal sandwich cell configuration because the metallic electrodes were not transparent. Therefore, the sensitized electrode was placed in a beaker facing the light and a Pt counter electrode was positioned at its side perpendicular to it. Photopotentials were measured in each of three CH_3CN solutions containing 0.5 M LiI; 0.05 M ferrocene and 0.1 M LiClO_4 ; or 0.05 M hydroquinone and 0.1 M LiClO_4 . The solution potentials were measured both before and after each experiment and the average value was used in the calculations. The potential was more positive after the experiments by 50–70 mV because of the generation of some of the oxidized half of the redox couple.

Results and Discussion

The use of only the reduced half of the redox couple prevents the dissolution of the gold substrate electrodes in I_3^- solution and also substantially slows the rate of the recombination reaction at the substrate (eqs 1) and at the TiO_2 surface.



The conventional dye cell uses I^-/I_3^- as the redox couple, and no other known redox couple works nearly as well. The use of most other redox couples, and most substrates besides SnO_2 , is expected to accelerate the recombination reactions relative to the conventional dye cell and thus diminish V_{oc} (independent of the mechanistic model). This would tend to obscure what we are looking for: the relation between $\Phi_{\text{sub}} - \Phi_{\text{redox}}$ and V_{oc} . Therefore we use only the reduced half of the redox couple to minimize recombination rates and maximize V_{oc} . This means that the photocurrent is concentration-limited at the counter electrode by the small amount of the oxidized half of the couple formed by the photoreaction and by thermal equilibration. Therefore, only the measured photovoltage in these

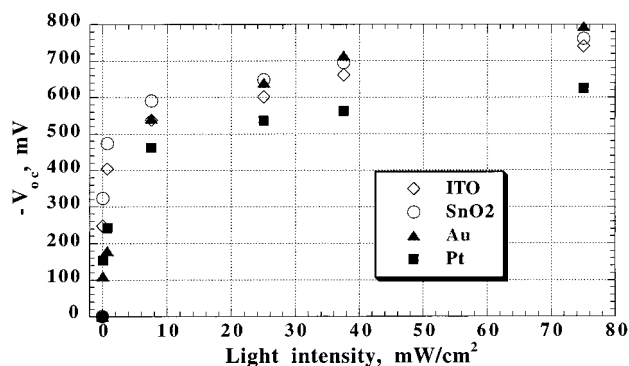


Figure 1. The open circuit photovoltage plotted vs incident light intensity for dye-sensitized TiO₂ films on each of the four types of substrate electrodes in 0.5 M LiI solution in acetonitrile.

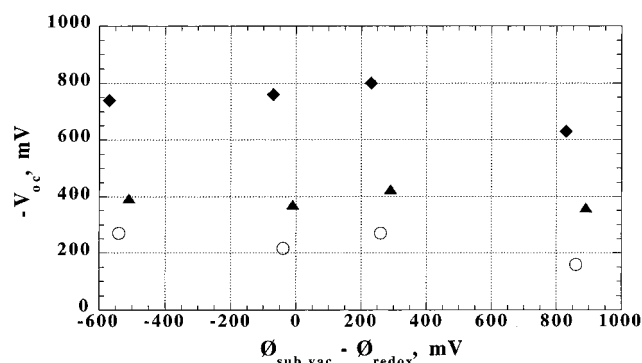


Figure 2. The open circuit photovoltage at 75 mW/cm² (~ 1 sun) plotted vs the difference between the work function of the substrate in vacuum, $\Phi_{\text{sub,vac}}$, and the solution redox potential, Φ_{redox} . The work function of the substrate in the solution, Φ_{sub} , the quantity of interest, is difficult to measure but is related to $\Phi_{\text{sub,vac}}$, see the discussion in the text. The four types of substrates are, from left to right, ITO, SnO₂, Au, and Pt; the filled diamonds are for 0.5 M LiI solution, the open circles are for 0.05 M ferrocene in 0.1 M LiClO₄ solution, and the filled triangles are for 0.05 M hydroquinone in 0.1 M LiClO₄ solution.

experiments, but not the photocurrent, contains fundamental information about the dye-sensitization process.

The experimentally determined photovoltages as a function of incident light intensity are shown in Figure 1 for the four substrate electrodes in 0.5 M LiI solution. V_{oc} increases approximately with the logarithm of the light intensity in all cases. There are no major differences between the magnitudes of the photovoltages on the different substrate electrodes despite the ~ 1.4 V range in their vacuum work functions. The slight decrease in V_{oc} on Pt substrates is probably caused by the enhanced rate of recombination (eq 1a) at this highly catalytic electrode. Supporting this interpretation is the observation that adding a small amount of I₂ to the solution, which might be expected to increase V_{oc} by shifting the solution potential positive, in fact greatly decreases it.

The measured photovoltages at 1 sun intensity are plotted versus the difference between the vacuum work functions of the substrate electrode and the measured solution redox potentials, $\Phi_{\text{sub,vac}} - \Phi_{\text{redox}}$, in Figure 2 for the solutions containing I⁻, ferrocene, and hydroquinone. The average measured potential of the redox electrolyte containing I⁻ and a trace of I₃⁻ was $\Phi_{\text{redox}} = +0.12$ V vs SCE. To account for photovoltages of ~ -0.8 V at one sun, the junction model would require that the work function of the substrate electrode, Φ_{sub} , in I⁻ solution be at least as negative as ~ -0.75 V vs SCE or approximately 4.0 V vs vacuum. Thus Φ_{sub} for each substrate in I⁻ solution would have to be more negative than the vacuum work function of In

or Al to explain the photovoltages with the junction model. It is difficult to know the actual work function of an electrode in solution, Φ_{sub} , the quantity that is predicted by the junction model to control the photovoltage, because the effects of double-layer charging and specific adsorption of ions are not known exactly. For example, I⁻ in aqueous NaClO₄ solution is known to specifically adsorb to Au as an anion and shift its point of zero charge (related to its work function) 0.8 V negative of its value in pure NaClO₄ solution.³² However, I⁻ specifically adsorbs in its neutral form, rather than as an anion, on Pt and thus a much smaller change of its effective work function is expected.³³ Coupled with the fact that $\Phi_{\text{sub,vac}}$ of Pt is 0.6 V positive of Au, this strongly suggests that $\Phi_{\text{sub}} - \Phi_{\text{redox}}$ for Pt substrates in I⁻ solution is a positive quantity. Nevertheless, a negative photovoltage of -0.63 V is measured. Little is known about the work functions of the oxide substrates in I⁻ solution.

We also measured the photovoltages of a series of fresh electrodes in ferrocene-containing solution (Figure 2) in order to avoid the ambiguities caused by specific adsorption of iodide ions. The average potential of this solution was $\Phi_{\text{redox}} \approx 0.09$ V vs SCE. In this solution, the double layer at the solution/substrate interface should be dominated by nonspecifically adsorbed solvent and LiClO₄ electrolyte and be only slightly perturbed by the large, outer-sphere redox couple. Therefore we expect much smaller shifts in Φ_{sub} from the vacuum values compared to I⁻ solution. The V_{oc} values measured in ferrocene solution were uniformly smaller than in I⁻ solution, as expected from the very fast electron exchange kinetics of the ferrocene species. Addition of a small amount of the oxidized form of ferrocene to the solution resulted in $V_{\text{oc}} \approx 0.0$ V, even for SnO₂ substrates, because of the rapid recombination reaction (eq 1b). But in solutions with no purposely added ferricenium, photovoltages of around -0.2 V were obtained for all substrates. To account for this, the junction model would require that the work function of each substrate electrode, Φ_{sub} , in ferrocene solution be ~ -0.15 V vs SCE (~ 4.6 V vs vacuum) or more negative.

Similar experiments with fresh electrodes were carried out in hydroquinone-containing solution ($\Phi_{\text{redox}} \approx 0.06$ V, Figure 2). Again, we expect much smaller deviations of Φ_{sub} from the vacuum values in this solution compared to I⁻ solution, and again we observe no significant variation of V_{oc} with substrate: $V_{\text{oc}} \approx -0.4$ V for all substrates. To account for this, the junction model would require that the work function of each substrate electrode in hydroquinone solution be ~ -0.38 V vs SCE (~ 4.4 V vs vacuum) or more negative.

There are unavoidable ambiguities in the values of $\Phi_{\text{sub}} - \Phi_{\text{redox}}$ in these experiments, but the overwhelming weight of the evidence points to a simple conclusion: V_{oc} is independent of $\Phi_{\text{sub}} - \Phi_{\text{redox}}$, and therefore the junction model is incorrect. To claim otherwise would require assuming that four different substrates, with widely varying vacuum work functions and interface chemistries, all converge to the same effective work function in three different solution environments. This seems nearly impossible. Therefore, we conclude that the photovoltage in dye cells is not determined by the equilibrium junction potential at the TiO₂/substrate interface.

The fact that the photovoltages are nearly independent of the work function of the substrate electrodes suggests that no significant junction potential occurs along the pathway that electrons follow from the bulk TiO₂ film to the substrate. This is somewhat surprising since an interfacial potential difference must occur upon equilibration of the substrate electrode with the electrolyte solution,^{12,24,26} and a substantial fraction of the potential should drop across the semiconductor. Of course, the

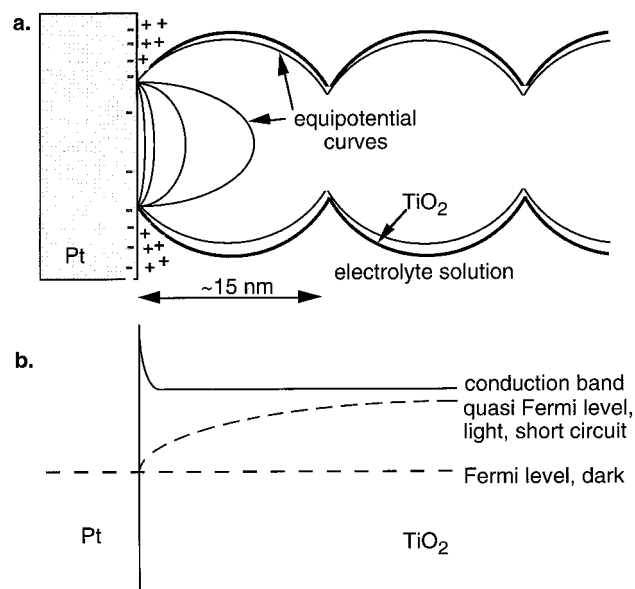


Figure 3. (a) Diagram showing qualitatively the spatial variation in the interfacial potential expected at an unreconstructed TiO₂/Pt interface. Only the ions involved in forming the interfacial electric field are shown, not the screening ions. This interface should present a barrier to electron transfer, but experimentally the barrier appears insignificant. It may be so thin near the particle surface that electrons can tunnel through it. (b) Approximate energy level diagram showing the narrow barrier near the particle surface at the TiO₂/Pt interface.

barrier in an actual dye cell, $\phi_{\text{sub}} - \phi_{\text{redox}}$, may be smaller than the barrier expected from measurements of clean substrates in UHV, $\phi_{\text{sub, vac}} - \phi_{\text{redox}}$, but the trend in barrier heights over a range of substrates is expected to remain. When ITO or SnO₂ substrates are used, both the “kinetic” factor (chemical potential gradient) and the electrical potential difference at the junction should drive electrons in the same direction, so it is difficult to distinguish between the two forces. But with a Pt substrate, the junction potential must oppose electron transfer from the TiO₂ into the substrate; so this case shows clearly that the junction barrier has almost no effect on the electron-transfer process. The reason for this is not yet understood. We propose two possible explanations: (1) the barrier may be so thin that electrons can tunnel through it; and/or (2) the high electric field ($\sim 10^6$ V/cm) at the unreconstructed interface may drive a chemical modification of the interphase leading to a smaller barrier height.

To understand the nature of the barrier at the TiO₂/Pt interface (taken as the most extreme, and therefore most instructive, example), it is necessary to consider the complex geometry of these cells and the corresponding spatial variations in the interfacial potential. We do not attempt to provide anything more than a qualitative description of these complicated interfaces (Figure 3). Some detailed calculations on a model system have recently been performed by Bisquert et al.²⁶ The TiO₂ film is made up of particles approximately 15 nm in diameter sintered together on a substrate electrode, leaving 40–50% of the film volume open. The electrolyte solution permeates the entire TiO₂ film through these voids, making direct contact with the substrate electrode over a substantial area. We suggest that the presence of electrolyte solution right up to the substrate electrode invalidates critical assumptions implicit in the junction model.

A small section of the TiO₂/electrolyte/Pt substrate interface is shown schematically in Figure 3. Since ϕ_{Pt} should be well positive of ϕ_{redox} , the Pt substrate will charge negative upon equilibration with the solution. This will attract positive ions

(Li⁺ in our experiments) to counterbalance the charge on the substrate. Because of the direct contact between the solution and the substrate, the electric field resulting from this double layer of charge will drop over a very short distance (in the Helmholtz layer). Since the solution is highly conductive, we assume that the surface of the TiO₂ exposed to it must approximate an equipotential surface.^{12,26} The interfacial electric field cannot penetrate far into the TiO₂ because the cations in solution can get very close to the substrate, relative to the particle diameter, and thus screen the field. Using these considerations, we have drawn, in a purely qualitative fashion, a set of expected equipotential curves at the TiO₂/Pt interface showing the highly nonuniform spatial distribution of the interfacial field in the TiO₂ particle (Figure 3). It appears that, at its widest point, the interfacial barrier may be somewhat less than the diameter of one particle. But if the electrons were to move mainly near the particle surface, as expected, close to their screening ions, they would experience an interfacial electric field that would drop over a distance only slightly wider than the Helmholtz layer, around 1 nm. (Although spatial variations in the interfacial barrier width were not discussed by Bisquert et al.,²⁶ our qualitative treatment appears to be consistent with their calculations. Schwarzburg and Willig apparently calculated the potential distribution only in one dimension through the middle of the particles.¹²) Electrons may be able to tunnel readily through such a thin barrier. Tunneling becomes appreciable for barriers less than 10–20 nm wide, and thermally assisted tunneling can be significant for barriers up to 200 nm wide.³⁴ Therefore, the ~ 1 nm wide junction expected at the TiO₂/solution/substrate interface in a dye cell may present no significant barrier to electron transfer in the case of electropositive substrates such as Pt and Au, and correspondingly, provide little significant assistance to electron transfer in the case of electronegative substrates such as ITO and SnO₂.

A related possibility is that the free energy contained in the high electric field at the TiO₂/Pt interface ($\sim 10^6$ V/cm) would drive a chemical modification (reconstruction) of the interphase. For example, reduction of the TiO₂ near the Pt and intercalation of Li⁺ to neutralize the resulting charge would lower the barrier height and thereby decrease the free energy of the system. Charging of surface states might have a similar effect. In fact, it seems unlikely that such a high electric field could exist in the presence of an electrolyte solution and a permittable, imperfect TiO₂ particle. One or both of these possibilities may explain the independence of V_{oc} from $\phi_{\text{sub}} - \phi_{\text{redox}}$.

The junction model postulates the need for an interfacial potential to separate the screened electron from its image charge in solution before the electron can move into the substrate electrode.¹² Our experiments show that no such potential is required for this process and, in fact, that charge separation occurs even in the presence of an interfacial potential of the wrong polarity. The fact that the TiO₂ particles at the TiO₂/substrate interface are surrounded (approximately) by electrolyte solution has two important consequences that seem to invalidate the assumptions of the junction model: (1) it limits the spatial extent of the interfacial electric field to nanoscopic dimensions, and thereby may also limit its magnitude, as discussed above; and (2) the photoinjected electrons will be electrostatically screened right up to the substrate electrode, so their transfer into the substrate will not result in the creation of a significant image charge field that would oppose charge transfer. Both the electron and the I₃[−] ion are electrostatically screened by cations such as Li⁺ in solution; but this screening, per se, presents no significant barrier to discharge at the electrodes.

The junction model may be important for understanding a possible variation of the dye cell. As discussed earlier, when the distance between the two layers of opposite charge (Figure 3a) is substantially smaller than the diameter of the TiO_2 particles, as it is in the normal dye cell, the electric field resulting from $\Phi_{\text{sub}} - \Phi_{\text{redox}}$ may be smaller than expected due to interphase reconstruction and/or may drop over such a small distance that it does not influence electron transfer across the interface. However, when the distance between the two charge layers becomes substantially greater, that is, when solvent is excluded from contact with the substrate electrode, the quantity $\Phi_{\text{sub}} - \Phi_{\text{redox}}$ should begin to influence the functioning of the solar cell. One way to achieve this is to deposit a pinhole-free, solid film of TiO_2 on the substrate before application of the nanocrystalline TiO_2 layer. (This is difficult, but it may be advantageous in suppressing the recombination reaction at the substrate when using a redox couple more kinetically facile than I^-/I_3^- .)³⁵ One consequence of a solid layer of TiO_2 interposed between the substrate and the nanocrystalline TiO_2 film would be the generation of an electric field (image force) between the electrons injected into the solid film and the screening ions left behind in solution.^{9,22,23} This field would oppose charge separation. Therefore, an electrical potential gradient (band bending) that promoted charge separation would be required for efficient electron conduction through the solid part of the TiO_2 film. (Such a favorable potential gradient may exist with ITO or SnO_2 substrates, but not with Au or Pt substrates.) The junction model, in fact, seems to apply more to this case than to the existing dye cells. However, even in this case, we believe that $\Phi_{\text{sub}} - \Phi_{\text{redox}}$ does not set an upper limit to V_{oc} because this notion denies the fact that a photoinduced chemical potential gradient, by itself, is sufficient to generate a photovoltage. The upper limit to V_{oc} is set by the photoinduced difference between the quasi Fermi levels of electrons and holes, not by the equilibrium electric field alone.

In summary, we have shown that the photovoltage in a dye-sensitized solar cell is not controlled by the dark interfacial electrical potential difference, in contrast to the prediction of the junction model. Rather, the photovoltage is nearly independent of the work function of the substrate electrode, in agreement with the kinetic model. Nevertheless, the junction model pointed out a possible deficiency in the kinetic model—its neglect of the equilibrium interfacial potential barrier. It turns out that this barrier is of no importance in the operation of the conventional dye cell, but it may become important if a nonporous TiO_2 film is interposed between the substrate and the nanocrystalline TiO_2 film. No junction potential of significant magnitude and spatial extent is expected at the TiO_2 /substrate interface in conventional dye cells because electrolyte permeates the entire TiO_2 film. The photovoltaic effect in these solar cells appears to be driven almost entirely by photoinduced chemical potential gradients; electrical junctions play no significant role.

Acknowledgment. We are grateful to Professor Frank Willig for valuable discussions about the junction model, and to the U.S. Department of Energy, Office of Science, Division of Basic

Energy Sciences, Chemical Sciences Division (BG) and Office of Utility Technologies, Division of Photovoltaics (F.P.) for supporting this research.

References and Notes

- (1) O'Regan, B.; Moser, J.; Anderson, M.; Grätzel, M. *J. Phys. Chem.* **1990**, *94*, 8720–8726.
- (2) O'Regan, B.; Grätzel, M. *Nature* **1991**, *353*, 737–740.
- (3) Kalyanasundaram, K.; Grätzel, M. *Coord. Chem. Rev.* **1998**, *77*, 347–414.
- (4) Nazeeruddin, M. K.; Kay, A.; Rodicio, I.; Humphry-Baker, R.; Müller, E.; Liska, P.; Vlachopoulos, N.; Grätzel, M. *J. Am. Chem. Soc.* **1993**, *115*, 6382–6390.
- (5) Parkinson, B. A.; Spitler, M. T. *Electrochim. Acta* **1992**, *37*, 943–948.
- (6) Södergren, A.; Hagfeldt, A.; Olsson, J.; Lindquist, S.-E. *J. Phys. Chem.* **1994**, *98*, 5552–5556.
- (7) Hagfeldt, A.; Lindquist, S.-E.; Grätzel, M. *Sol. Energy Mater. Sol. Cells* **1994**, *32*, 245–257.
- (8) Cao, F.; Oskam, G.; Meyer, G. J.; Searson, P. C. *J. Phys. Chem.* **1996**, *100*, 17021–17027.
- (9) Zaban, A.; Meier, A.; Gregg, B. A. *J. Phys. Chem. B* **1997**, *101*, 7985–7990.
- (10) de Jongh, P. E.; Vanmaekelbergh, D. *J. Phys. Chem. B* **1997**, *101*, 2716–2722.
- (11) Solbrand, A.; Lindström, H.; Rensmo, H.; Hagfeldt, A.; Lindquist, S.-E.; Södergren, S. *J. Phys. Chem. B* **1997**, *101*, 2514–2518.
- (12) Schwarzburg, K.; Willig, F. *J. Phys. Chem. B* **1999**, *103*, 5743–5746.
- (13) Hodes, G.; Howell, I. D. J.; Peter, L. M. *J. Electrochem. Soc.* **1992**, *139*, 3136–3140.
- (14) Boschloo, G. K.; Goossens, A.; Schoonman, J. *J. Electroanal. Chem.* **1997**, *428*, 25–32.
- (15) Ferber, J.; Stangl, R.; Luther, J. *Sol. Energy Mater. Sol. Cells* **1998**, *53*, 29–54.
- (16) Enright, B.; Fitzmaurice, D. *J. Phys. Chem.* **1996**, *100*, 1027–1035.
- (17) Kamat, P. V.; Bedja, I.; Hotchandani, S.; Patterson, L. K. *J. Phys. Chem.* **1996**, *100*, 4900–4908.
- (18) Zaban, A.; Ferrere, S.; Gregg, B. A. *J. Phys. Chem. B* **1998**, *102*, 452–460.
- (19) Schlichthörl, G.; Huang, S. Y.; Sprague, J.; Frank, A. J. *J. Phys. Chem. B* **1997**, *101*, 8141–8155.
- (20) Franco, G.; Gehring, J.; Peter, L. M.; Ponomarev, E. A.; Uhlenndorf, I. *J. Phys. Chem. B* **1999**, *103*, 692–698.
- (21) Dloczik, L.; Ieperuma, O.; Lauermann, I.; Peter, L. M.; Ponomarev, E. A.; Redmond, G.; Shaw, N. J.; Uhlenndorf, I. *J. Phys. Chem. B* **1997**, *101*, 10281–10289.
- (22) Charlé, K.-P.; Willig, F. *Chem. Phys. Lett.* **1978**, *57*, 253–258.
- (23) Spitler, M. T. *J. Electroanal. Chem.* **1987**, *228*, 69–76.
- (24) Nozik, A. J.; Memming, R. *J. Phys. Chem.* **1996**, *100*, 13061–13078.
- (25) Levy, B.; Liu, W.; Gilbert, S. E. *J. Phys. Chem. B* **1997**, *101*, 1810–1816.
- (26) Bisquert, J.; Garcia-Belmonte, G.; Fabregat-Santiago, F. *J. Solid State Electrochem.* **1999**, *3*, 337–348.
- (27) Dittrich, T.; Beer, P.; Koch, F.; Weidmann, J.; Lauermann, I. *Appl. Phys. Lett.* **1998**, *73*, 1901–1903.
- (28) Grovenor, C. R. M. *Microelectronic Materials*; IOP Publishing: Bristol, 1989.
- (29) *CRC Handbook of Chemistry and Physics*, 61 ed.; Weast, R. C., Ed.; CRC Press: Boca Raton, 1980.
- (30) Zaban, A.; Ferrere, S.; Sprague, J.; Gregg, B. A. *J. Phys. Chem. B* **1997**, *101*, 55–57.
- (31) Pichot, F.; Ferrere, S.; Pitts, R. J.; Gregg, B. A. *J. Electrochem. Soc.* **1999**, *146* (11), 4324–4326.
- (32) Ueno, K.; Seo, M. *J. Electrochem. Soc.* **1999**, *146*, 1496–1499.
- (33) Lane, R. F.; Hubbard, A. T. *J. Phys. Chem.* **1975**, *79*, 808–815.
- (34) Fahrenbruch, A. L.; Bube, R. H. *Fundamentals of Solar Cells. Photovoltaic Solar Energy Conversion*; Academic Press: New York, 1983.
- (35) Bach, U.; Lupo, D.; Comte, P.; Moser, J. E.; Weissörtel, F.; Salbeck, J.; Spreitzer, H.; Grätzel, M. *Nature* **1998**, *395*, 583–585.